Fine-Tuning of Photosynthesis Requires CURVATURE THYLAKOID1-Mediated Thylakoid Plasticity[1]

Mathias Pribil,[a,b,2,3] Omar Sandoval-Ibáñez,[b,2] Wenteng Xu,[a,2,4] Anurag Sharma,[b] Mathias Labs,[a] Qiuping Liu,[a,5] Carolina Galgenmüller,[a,b] Trang Schneider,[c] Malgorzata Wessels,[d] Shizue Matsubara,[c] Stefan Jansson,[d] Gerhard Wanner,[a] and Dario Leister[a]

[a]Plant Molecular Biology (Botany), Department Biology I, Ludwig-Maximilians-Universität München, 82152 Planegg-Martinsried, Germany
[b]Copenhagen Plant Science Centre, Department of Plant and Environmental Sciences, University of Copenhagen, DK-1871 Frederiksberg C, Copenhagen, Denmark
[c]Institut für Pflanzenwissenschaften, Forschungszentrum Jülich, 52425 Juelich, Germany
[d]Umeå Plant Science Centre, Department of Plant Physiology, Umeå University, 901 87 Umea, Sweden

ORCID IDs: 0000-0002-9174-9548 (M.P.); 0000-0002-4513-1704 (O.S.-I.); 0000-0003-3887-9973 (W.X.); 0000-0001-5345-8830 (A.S.); 0000-0001-6436-9585 (M.W.); 0000-0002-1440-6496 (S.M.); 0000-0002-7906-6891 (S.J.); 0000-0002-5996-5902 (G.W.); 0000-0003-1897-8421 (D.L.).

The thylakoid membrane system of higher plant chloroplasts consists of interconnected subdomains of appressed and nonappressed membrane bilayers, known as grana and stroma lamellae, respectively. CURVATURE THYLAKOID1 (CURT1) protein complexes mediate the shape of grana stacks in a dosage-dependent manner and facilitate membrane curvature at the grana margins, the interface between grana and stroma lamellae. Although grana stacks are highly conserved among land plants, the functional relevance of grana stacking remains unclear. Here, we show that inhibiting CURT1-mediated alteration of thylakoid ultrastructure in Arabidopsis (*Arabidopsis thaliana*) reduces photosynthetic efficiency and plant fitness under adverse, controlled, and natural light conditions. Plants that lack CURT1 show less adjustment of grana diameter, which compromises regulatory mechanisms like the photosystem II repair cycle and state transitions. Interestingly, CURT1A suffices to induce thylakoid membrane curvature in planta and thylakoid hyperbending in plants overexpressing CURT1A. We suggest that CURT1 oligomerization is regulated at the posttranslational level in a light-dependent fashion and that CURT1-mediated thylakoid plasticity plays an important role in fine-tuning photosynthesis and plant fitness during challenging growth conditions.

The thylakoid membrane system in the chloroplasts of higher plants is typically organized into a three-dimensional network of cylindrical substructures composed of stacked membrane sheets, which show a conserved average diameter of 300 to 600 nm (Mustárdy and Garab, 2003; Mullineaux, 2005; Anderson et al., 2008; Kirchhoff, 2008). These so-called grana stacks are interconnected by unstacked membrane sheets, the stroma lamellae, forming a continuous membrane system that encloses a single, continuous lumenal space (Shimoni et al., 2005; Armbruster et al., 2013; Kirchhoff, 2013a; Pribil et al., 2014). Grana and stroma lamellae differ significantly in their protein composition, displaying lateral heterogeneity (Andersson and Anderson, 1980; Albertsson, 2001; Dekker and Boekema, 2005; Nevo et al., 2012; Kirchhoff, 2013a). PSII and light-harvesting complex II (LHCII) are preferentially located in the stacked membranes of grana, where they form supercomplexes and megacomplexes. In contrast, PSI, LHCI, and the ATP synthase congregate within the unstacked stroma lamellae and grana end membranes. The localization of the cytochrome b_6f complex (Cyt b_6f) is less clear, but it is likely dispersed across both appressed and nonappressed regions of the thylakoids (Dekker and Boekema, 2005; Nevo et al., 2012).

The thylakoid membrane is an extremely dynamic and flexible system that shows a high degree of plasticity, especially when exposed to adverse environmental conditions, such as high or fluctuating light

[1] M.P. and D.L. thank the Deutsche Forschungsgemeinschaft (FOR2092 and TRR 175 project C05) and S.J. the Swedish Research Council for financial support. M.P. further acknowledges financial support from Copenhagen Plant Science Centre funded by the University of Copenhagen and the Novo Nordisk Foundation (NNF15OC0016586). A.S. thanks Carlsbergfondet for financial support.

[2] These authors contributed equally to the article.

[3] Address correspondence to pribil@plen.ku.dk.

[4] Current address: Yellow Sea Fisheries Research Institute, Chinese Academy of Fishery Sciences, Qingdao 266071, China.

[5] Current address: Laboratory of Natural Products Pesticides, College of Plant Protection, Southwest University, Chongqing 400716, China.

The author responsible for distribution of materials integral to the findings presented in this article in accordance with the policy described in the Instructions for Authors (www.plantphysiol.org) is: Mathias Pribil (pribil@plen.ku.dk).

W.X., O.S.-I., M.L., A.S., Q.L., C.G., T.S., M.W., S.M., G.W., and M.P. conducted the experiments; M.P., D.L., W.X., O.S.-I., A.S., M.L., S.M., and S.J. designed the experiments; M.P., W.X., O.S.-I., A.S., and D.L. wrote and reviewed the article; D.L and M.P. secured funding.

www.plantphysiol.org/cgi/doi/10.1104/pp.17.00863

intensities. For instance, grana numbers increase under low-light conditions (Anderson, 1986), and high light intensities reduce grana diameter and cause partial transverse unstacking of grana membranes (Fristedt et al., 2009; Khatoon et al., 2009; Herbstová et al., 2012; Yoshioka-Nishimura et al., 2014). In photodamaging light conditions, the decrease in grana diameter is thought to facilitate PSII repair by providing the FtsH protease, involved in D1 degradation, easier access to damaged PSII complexes located in the grana stacks (Kirchhoff, 2013b; Pribil et al., 2014). Hence, lateral shrinkage of grana diameter is assumed to accelerate the diffusion of damaged D1 proteins from the grana core to the stroma lamellae, expediting their turnover (Herbstová et al., 2012; Kirchhoff, 2014a, 2014b). Under low-light conditions, the structural conformation of the thylakoid membrane would tend to exclude FtsH from the grana core by steric hindrance (Kirchhoff, 2013a).

The small protein family CURVATURE THYLAKOID1 (CURT1) has been proposed to mediate the tight bending of the thylakoid membrane at the grana margins (Armbruster et al., 2013). Membrane bending is a prerequisite for defined grana formation and is facilitated by CURT1 proteins in a quantity-dependent manner. Grana of CURT1A-overexpressor lines (oe*CURT1A*) were found to have a reduced diameter and to contain more membrane layers, whereas grana of the quadruple CURT1 mutant (*curt1abcd*) showed an increased and strongly variable diameter (Armbruster et al., 2013). Traditionally, it was thought that perturbation of the conserved substructure of grana and stroma lamellae should have a significant impact on photosynthesis (Dörmann et al., 1995; Meurer et al., 1998; Gao et al., 2006; Kwon and Cho, 2008; Cui et al., 2011). However, CURT1 mutants grown under controlled conditions (CC) exhibited only moderate effects on photosynthetic performance (Armbruster et al., 2013). In this study, we further investigated the role of CURT1-mediated thylakoid plasticity in the regulation of photosynthesis during variable and stressful light conditions. Our data suggest that CURT1-mediated thylakoid plasticity contributes to thylakoid ultrastructure reorganization and is required for photosynthetic efficiency and overall plant fitness.

RESULTS

Dearth of CURT1 Negatively Affects Photosynthesis, Particularly under High-Light Conditions

Perturbation of the highly conserved structural heterogeneity of thylakoid membranes with distinct stacked grana and nonstacked stroma lamellae fractions in higher plants would be expected, a priori, to have a marked impact on photosynthesis. However, a reduction of CURT1 proteins associated with significant thylakoid ultrastructure alterations was shown previously to have only a moderate and pleiotropic impact on photosynthesis in Arabidopsis (*Arabidopsis thaliana*; Armbruster et al., 2013). As yet, no systematic assessment investigating the effects of CURT1 protein knockout or overexpression on photosynthesis and plant growth under different environmental growth conditions has been undertaken. To remedy this, the wild-type ecotype Landsberg *erecta* (L*er*), the quadruple CURT1 mutant *curt1abcd*, and oe*CURT1A* plants were grown on different day/night cycles (short, intermediate, and long days) and under different light intensities (low [LL], growth [GL], and high light [HL]) as well as in fluctuating light conditions. As shown previously, *curt1abcd* plants displayed decreases in the effective quantum yield (Φ_{II}) and nonphotochemical quenching (NPQ) and an increase in excitation pressure (1-qL) under GL conditions (120 μmol photons m^{-2} s^{-1}), whereas the functionality of PSII (F_v/F_m) was only weakly affected (Fig. 1A; Armbruster et al., 2013). Interestingly, oe*CURT1A* plants showed slightly reduced F_v/F_m values when grown under GL and LL conditions (Fig. 1A). However, no severe differences in Φ_{II}, 1-qL, or NPQ could be observed between wild-type and oe*CURT1A* plants under LL, GL, or HL conditions, suggesting effective regulation of photosynthesis under the given growth conditions. This inference is further supported by a wild-type-like effectiveness of the state transition mechanism (qT) in oe*CURT1A* (0.13 ± 0.04) versus the wild type (0.1 ± 0.02), showing similar transition kinetics to those determined by 77K fluorescence emission measurements (Fig. 1B). In contrast, *curt1abcd* displayed a marked delay in the transition kinetics from state 1 to state 2 (Fig. 1B), which is in line with a reduced qT value of 0.04 ± 0.01. In fact, qT was determined based on measurements performed 15 min after exposure to the respective state 1 or state 2 light conditions, suggesting an incomplete relocation of LHCII between the photosystems in the case of *curt1abcd*.

When plants were grown under HL conditions, both F_v/F_m and Φ_{II} were reduced significantly in *curt1abcd* plants relative to the wild type, whereas oe*CURT1A* showed wild-type-like values (Fig. 1A). This suggests a critical role of CURT1-dependent thylakoid plasticity in maintaining photosynthetic efficiency under challenging light conditions. To determine the extent to which a potentially perturbed D1 repair mechanism might contribute to photoinhibition in *curt1abcd* under HL conditions, the rate of D1 degradation was assessed in wild-type, *curt1abcd*, and oe*CURT1A* lines. To this end, detached leaves from all three genotypes were preincubated in the presence or absence of lincomycin, to inhibit de novo D1 synthesis, and then exposed to HL for 3 h. D1 turnover was assessed indirectly by the functional state of PSII complexes based on the F_v/F_m value. In both *curt1abcd* and oe*CURT1A* lines, D1 repair seemed to be impaired compared with the wild type, which was indicated by a more pronounced and persistent decline in F_v/F_m after prolonged HL exposure (Fig. 1C, left). In the case of oe*CURT1A*, the decline in F_v/F_m was slightly less distinct but similarly failed to stabilize after 2 to 3 h of HL treatment as compared with

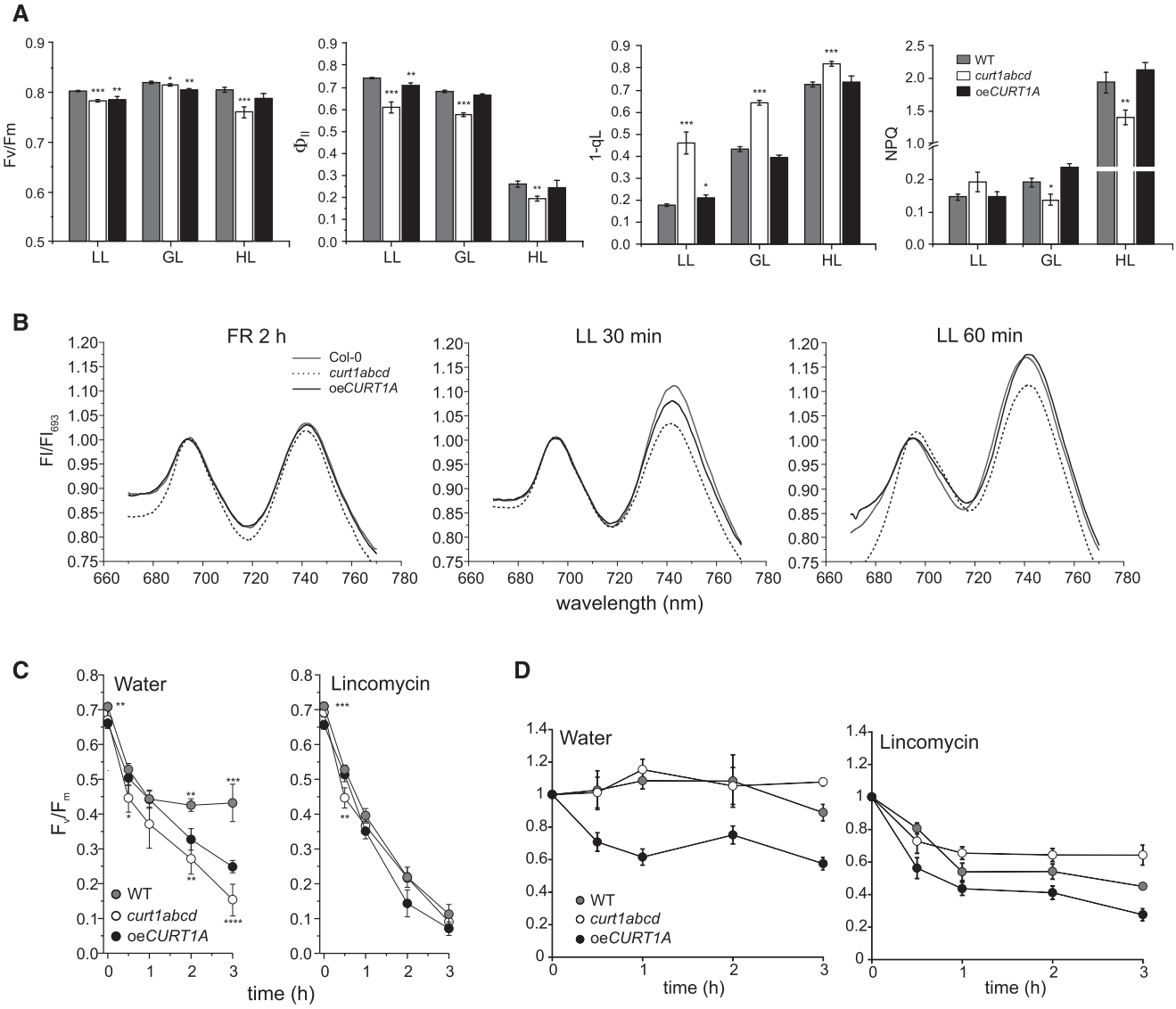

Figure 1. Effects of loss and overexpression of CURT1 on photosynthesis and acclimation processes. A, The photosynthetic parameters F_v/F_m, Φ_{II}, 1-qL, and NPQ were determined for Arabidopsis wild-type L*er* (WT), *curt1abcd*, and oe*CURT1A* lines grown under LL (30 μmol photons m^{-2} s^{-1}), GL (120 μmol photons m^{-2} s^{-1}), and HL (900 μmol photons m^{-2} s^{-1}) conditions in a 12-h/12-h light/dark photoperiod. To mimic the respective light treatments, the actinic light intensities for the pulse amplitude modulation (PAM) measurements were 39, 129, and 1,030 μmol photons m^{-2} s^{-1} for the plants grown under LL, GL, and HL, respectively. A two-sample Student's *t* test analysis ($P = 0.05$) was performed to determine the level of statistical significance; *P* values are represented by star code (*$P = 0.01$–0.05; **$P = 0.001$–0.01; and ***$P = 0.0001$–0.001 [$n = 7$]). B, Kinetics of state 1-to-state 2 transition measured by low-temperature (77K) fluorescence emission. Wild-type, *curt1abcd*, and oe*CURT1A* plants were acclimated for 2 h to far-red (FR) light followed by exposure to LL (80 μmol photons m^{-2} s^{-1}) to study the transition kinetics from state 1 to state 2. 77K fluorescence emission spectra were recorded at an excitation wavelength of 435 nm and normalized at 693 nm for direct comparison of the fluorescence emission peak deriving from PSI (743 nm). All depicted spectra represent averages of three biological replicates with five individual readings of each replicate. C, Photoinhibition in detached leaves of wild-type, *curt1abcd*, and oe*CURT1A* lines. PSII photoinhibition in the wild type, *curt1abcd*, and oe*CURT1A* was monitored by measuring the F_v/F_m value during HL exposure (3 h, 900 μmol photons m^{-2} s^{-1}) in the absence or presence of 1 mM lincomycin to inhibit D1 de novo synthesis. F_v/F_m measurements were performed at 0.5- or 1-h intervals ($n \geq 5$). Error bars represent SE. A two-sample Student's *t* test analysis ($P = 0.05$) was performed to determine the level of statistical significance; *P* values are represented by star code (*$P = 0.01$–0.05; **$P = 0.001$–0.01; ***$P = 0.0001$–0.001; and ****$P < 0.0001$). D, Graphs represent total D1 protein levels in the wild type, *curt1abcd*, and oe*CURT1A* during photoinhibition kinetics as described in C. Error bars represent SE ($n = 3$). Thylakoids were extracted from the same leaf material used to determine the F_v/F_m values shown in C. Thylakoids equivalent to 0.5 μg of chlorophyll were loaded in each lane. Western blotting was performed using a primary antibody specific against D1. Representative immunoblots are provided in Supplemental Figure S2.

the wild type. Interestingly, inhibition of D1 de novo synthesis by lincomycin treatment caused a similarly strong and prolonged decrease in F_v/F_m upon HL exposure in all three genotypes (Fig. 1C, right). This suggests that a hampered de novo synthesis of D1 protein or its improper integration into functional PSII complexes might be responsible for the reduced F_v/F_m observed in water-treated *curt1abcd* and oe*CURT1A* leaves (Fig. 1C, left). To assess whether the decrease in F_v/F_m could be associated with a reduced efficiency in D1 protein turnover, the accumulation of D1 was analyzed by western blotting in the same leaves treated with or without lincomycin. D1 degradation in *curt1abcd* was less efficient than in the wild type treated with lincomycin, which suggests that a grana architecture with increased diameter negatively affects D1 turnover and, thus, photosynthetic efficiency (Fig. 1D, right; Supplemental Fig. S2). Correspondingly, faster D1 degradation was observed in lincomycin-treated oe*CURT1A* leaves, which contain grana with reduced diameter (Fig. 1D, right; Supplemental Fig. S2). However, a sole increase in D1 degradation in oe*CURT1A* was not associated with an improved or wild-type-like ability to cope with short-term HL stress (Fig. 1, C and D). This suggests that the thylakoid hyperbending phenotype observed in oe*CURT1A* perturbs the PSII repair cycle by imposing restrictions on the reassembly of functional PSII rather than by limiting the degradation of damaged D1 protein. Alterations in the photoperiod had little or no additional effect on photosynthetic properties of *curt1abcd* and oe*CURT1A* plants cultivated at GL intensities. Both lines showed similar changes in photosynthetic parameters compared with the wild type across the different previously described photoperiods (Supplemental Fig. S1A).

Changes in CURT1 Levels Negatively Affect Plant Growth, Especially under Challenging Light Conditions

To assess the effect of the alteration of thylakoid ultrastructure on plant growth, relative growth rates (RGRs) were determined for wild-type (Col-0), *curt1abcd*, and oe*CURT1A* plants grown under fluctuating light conditions in comparison with controlled GL. Here, *curt1abcd* and oe*CURT1A* showed generally reduced RGRs compared with the wild type under both control and fluctuating light conditions (Table I). However, in terms of the relative change in RGR for each genotype under the different light conditions, *curt1abcd* plants showed a stronger decrease in RGR under fluctuating conditions than either wild-type or oe*CURT1A* plants (Table I).

Furthermore, the increase in rosette leaf area of wild-type, *curt1abcd*, and oe*CURT1A* plants was measured over 4 consecutive weeks of growth under the previously specified day/night cycles and light intensities. Both *curt1abcd* and oe*CURT1A* showed general reductions in the projected leaf area relative to the wild type, regardless of the light conditions or photoperiod employed (Supplemental Fig. S1, B–G). The reduction in leaf area in *curt1abcd* and oe*CURT1A* was particularly pronounced after 5 weeks of growth under LL (70% and 48% of the wild type, respectively) and HL (61% and 31% of the wild type, respectively; Supplemental Fig. S1, B and D). Similarly, a reduced photoperiod (short day) led to a marked reduction in plant growth, with projected leaf areas in 5-week-old *curt1abcd* and oe*CURT1A* plants corresponding to 52% and 48%, respectively, of the value for the wild type (Supplemental Fig. S1E). These observations suggest that, under adverse growth conditions, mutational alteration of the thylakoid ultrastructure negatively affects plant growth.

Table I. *Summary of the average RGR (% d^{-1}) of Arabidopsis wild-type (Col-0), curt1abcd, and oeCURT1A plants when cultivated under controlled light (CL) and fluctuating light (FL) conditions*

Average RGR values ± SD are shown ($n < 13$). RGR values were additionally normalized to the value in CL for each genotype.

Plant	RGR		RGR Normalized to CL	
	CL	FL	CL	FL
Wild type	18.8 ± 2.3	17.0 ± 2.4	1.00	0.90
curt1abcd	16.6 ± 0.5	13.8 ± 1.8	1.00	0.83
oe*CURT1A*	15.7 ± 2.0	15.1 ± 1.5	1.00	0.96

CURT1A Overaccumulation Does Not Alter Thylakoid Protein Composition and Is Primarily Responsible for Increased Membrane Bending

As shown previously, lack of CURT1 proteins does not affect the stoichiometry and assembly states of the major photosynthetic complexes (Armbruster et al., 2013), so another factor must be responsible for impairing the photosynthetic efficiency and plant growth seen in these mutants. However, the impact of CURT1A overaccumulation on thylakoid membrane complexes remains to be clarified. We analyzed the major photosynthetic protein complexes in the thylakoid membranes of wild-type and oe*CURT1A* plants by second-dimensional blue-native-PAGE (2D-BN-PAGE). As in the *curt1abcd* mutant, no major changes in the stoichiometry or assembly states of major photosynthetic protein complexes were observed in oe*CURT1A* plants relative to the wild type under GL conditions (Fig. 2A). Merely, a slightly increased PSI-LHCI-pLHCII-to-PSI-LHCI ratio was observed for oe*CURT1A* plants compared with the wild type (Fig. 2A). The assembly of CURT1A into higher molecular weight complexes in oe*CURT1A* lines when cultivated under GL was confirmed (Fig. 2A; Armbruster et al., 2013). As shown previously, knockout of CURT1A is associated with a decrease in the amounts of the other subunits of the CURT1 complex (Armbruster et al., 2013). To determine whether the ectopic overaccumulation of CURT1A also leads to changes in the

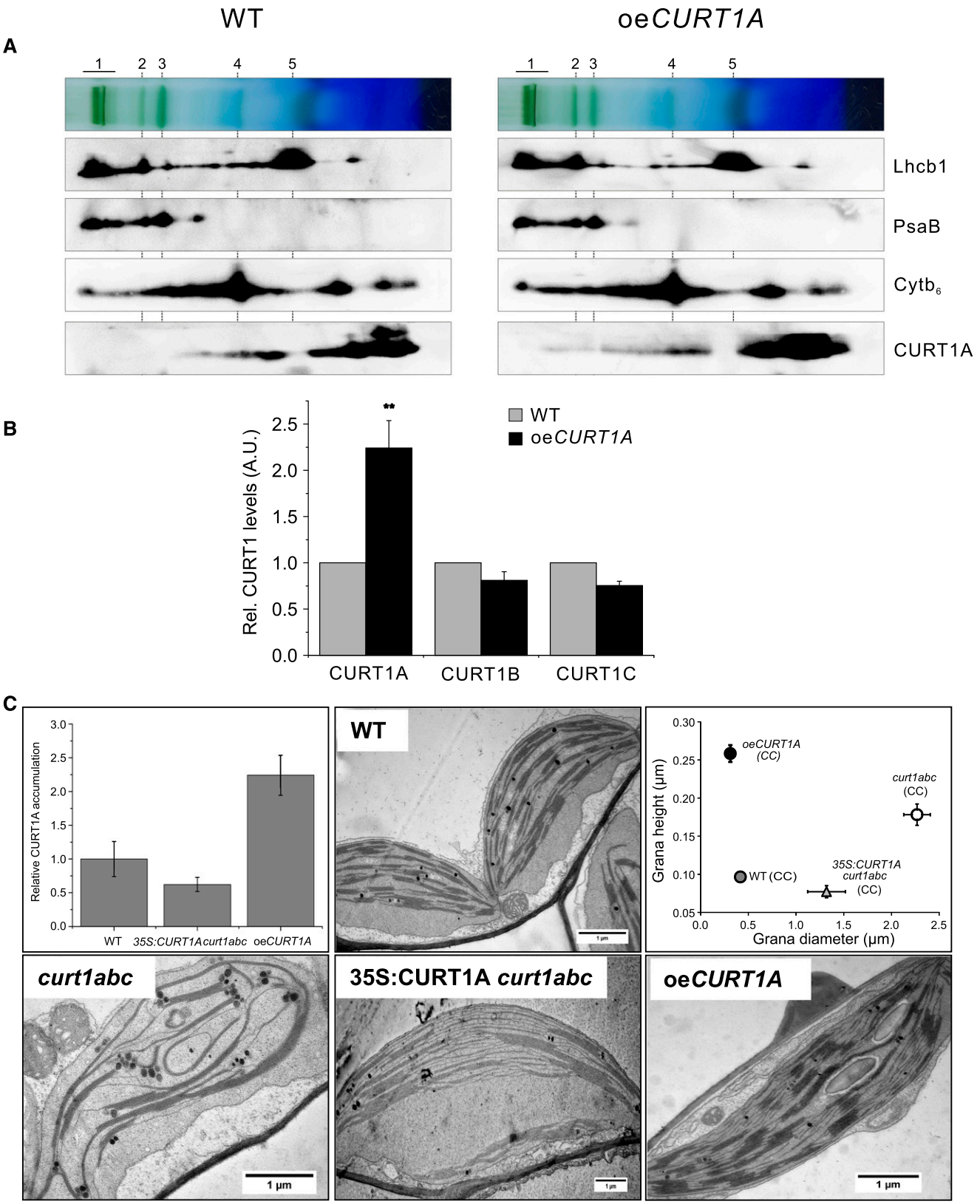

Figure 2. Overaccumulation of CURT1A alone results in increased thylakoid curvature but does not affect thylakoid protein complex composition. A, 2D-BN-PAGE of digitonin-solubilized thylakoids isolated from wild-type L*er* (WT) and oe*CURT1A* plants grown under GL conditions. Thylakoids equal to 50 μg of chlorophyll were loaded in each well for BN-PAGE. The major

accumulation of the remaining CURT1 proteins, levels of CURT1A, CURT1B, and CURT1C were quantified and compared between the wild type and oe*CURT1A* (Fig. 2B). Interestingly, under GL conditions, an ~2.5-fold increase in CURT1A in oe*CURT1A* was not accompanied by the up-regulation of any of the other CURT1 protein family members (Fig. 2B). This suggests that the increase in CURT1A alone accounts for the intensification in thylakoid membrane curvature observed in oe*CURT1A* plants (Armbruster et al., 2013). This is further supported by the fact that thylakoid curvature in CURT1 mutants (*curt1abc*) can be partially restored by ectopic expression of CURT1A (35S:CURT1A *curt1abc*), even when the levels attained are below those in the wild type (Fig. 2C). The comparison of the grana diameter observed in 35S:CURT1A *curt1abc* (~1.3 μm) and oe*CURT1A* lines (~0.4 μm) along with their CURT1A expression levels (60% and 250% of the wild type, respectively) suggests a strong correlation between CURT1A quantity and the plant's ability to mediate changes in grana diameter.

CURT1 Abundance, But Not Its Oligomerization State, Remains Stable during Short-Term Increases in Light Intensities

Plants exposed to HL intensity have been shown to decrease their grana diameter, which emphasizes the importance of thylakoid membrane plasticity under variable light conditions (Herbstová et al., 2012). To investigate whether changes in CURT1 protein amounts or their oligomerization might account for such structural rearrangements, wild-type and oe*CURT1A* plants were acclimated to darkness, GL, or HL, and CURT1 amounts as well as CURT1A-related oligomerization states were determined. Interestingly, CURT1 protein levels remained fairly stable during a 2-h exposure to different light intensities in both wild-type and oe*CURT1A* plants (Fig. 3A). However, with increasing light intensities, CURT1A complexes become progressively destabilized, resulting in a drastic decrease in high-molecular-weight (HMW) CURT1 complexes under solubilizing conditions, as shown by 2D-BN-PAGE (Fig. 3B). Due to the larger proportion of HMW CURT1 complexes in oe*CURT1A* (Armbruster et al., 2013), this tendency was more prominent in oe*CURT1A* than in wild-type plants.

A Lack of CURT1 Reduces Overall Plant Fitness and Seed Quality

As described above, *curt1abcd* and oe*CURT1A* plants both showed reduced growth under controlled adverse lighting conditions (i.e. LL, HL, fluctuating light, and short-day conditions; Table I). However, the extent to which alterations in thylakoid ultrastructure and thylakoid plasticity might affect overall plant fitness under natural environmental conditions has not been explored. Thus, randomized field trials were conducted in two consecutive years (2013 and 2014) with wild-type (Col-0), *curt1abcd*, and oe*CURT1A* plants, and plant fitness was determined based on seed production as described previously (Frenkel et al., 2008). Interestingly, overall seed production was severely affected in *curt1abcd* mutant plants (by ~85% relative to the wild type in 2013), while the fitness of oe*CURT1A* plants was less drastically affected, with a 15% reduction in total seed yield compared with the wild type in the same year (Fig. 4A). In 2014, comparable tendencies were observed for both experimental genotypes. In 2013 and 2014, the overall reduction in seed yield in *curt1abcd* and oe*CURT1A* was due primarily to a strong decrease in the number of siliques per plant rather than to the seed filling of the respective siliques (Fig. 4A). A reduced photosynthetic capacity as shown for *curt1abcd* was linked previously to a decrease in seed quality (Allorent et al., 2015). Thus, seed germination and viability assays were performed to analyze the effect of altered thylakoid ultrastructure on seed quality. Here, a lower rate of germination of *curt1abcd* seeds was observed compared with the wild type (Fig. 4B). However, no differences were detected for oe*CURT1A* plants, with seeds showing similar germination rates after 3 d (Fig. 4B). The same tendency was observed for cotyledon emergence (Fig. 4B). Due to the low germination rate exhibited in the *curt1abcd* mutant, we

Figure 2. (*Continued.*)
protein complexes separated by BN-PAGE are numbered and represent PSII supercomplexes (1), PSI-LHCI-pLHCII (2), PSI-LHCI (3), Cyt b_6f dimer (4), and LHCII trimer (5). Antibodies specific for Lhcb1, PsaB, $Cytb_{6f}$, and CURT1A were used to detect thylakoid protein complex assemblies after separation in the second dimension by SDS-PAGE. B, Quantification of CURT1 protein family members in oe*CURT1A*. Thylakoid preparations of wild-type and oe*CURT1A* plants were compared with respect to CURT1 levels by western-blot analysis using CURT1A-, CURT1B-, and CURT1C-specific antibodies ($n = 4$). A two-sample Student's t test analysis ($P = 0.05$) was performed to determine the level of statistical significance; P values are represented by star code (**$P = 0.001$–0.01). A.U., Arbitrary units. C, Top left, Comparison of CURT1A accumulation in the wild type, *curt1abc* mutants ectopically expressing CURT1A (35S:*CURT1A curt1abc*), and the line overexpressing CURT1A (oe*CURT1A*). Quantitative data of immunoblots ($n = 3$) using CURT1A-specific antibodies are shown. Thylakoids corresponding to 1 μg of chlorophyll were loaded. Top middle and bottom, TEM images of the thylakoid membrane system of chloroplasts derived from intact leaves of 4-week-old wild-type, *curt1abc* mutant, *curt1abc* mutant complemented with CURT1A (35S:CURT1A *curt1abc*), and oe*CURT1A* plants. Top right, Scatterplot showing the diameter (x axis) and height (y axis) of grana stacks in Arabidopsis wild-type, *curt1abc*, 35S:*CURT1A curt1abc*, and oe*CURT1A* plants grown under CC. Average values ± SE are presented ($n \geq 30$).

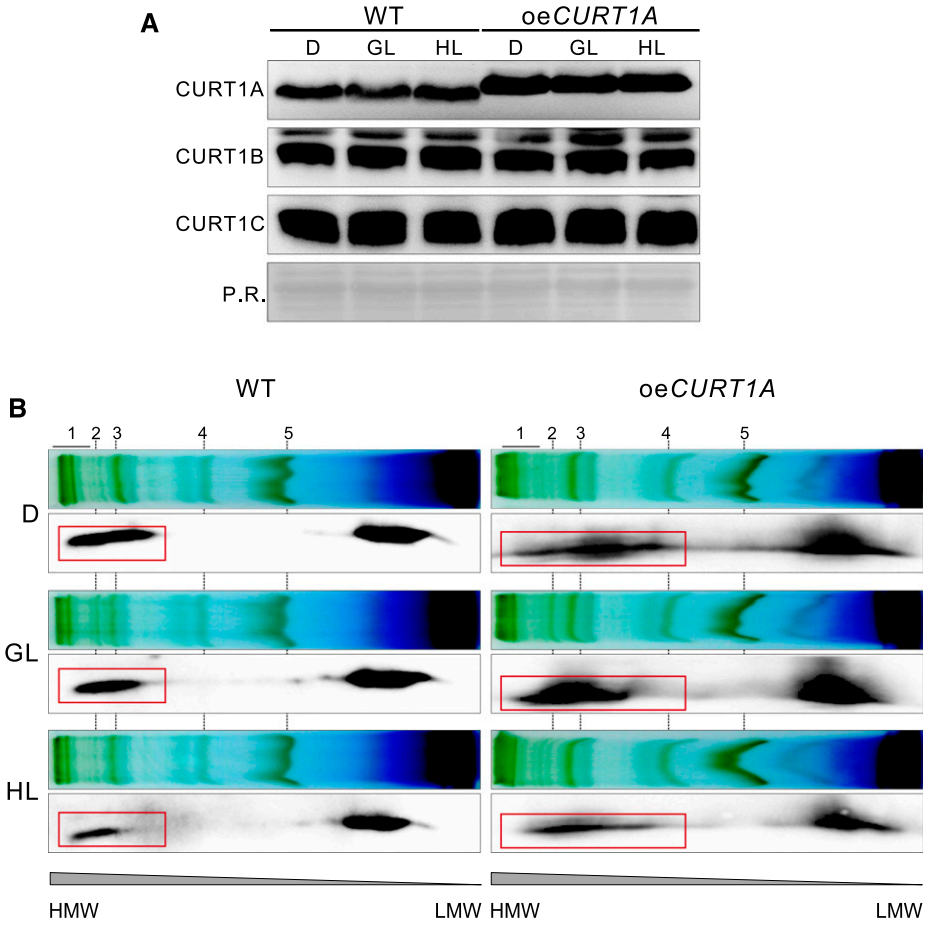

Figure 3. CURT1 protein levels, but not their oligomerization state, remain stable under increasing light intensities. A, Comparison of CURT1 protein amounts in oe*CURT1A* versus wild-type L*er* (WT) after 16 h of acclimation to darkness (D) followed by 2 h of either GL or HL exposure. Thylakoid protein composition was analyzed with CURT1A-, CURT1B-, and CURT1C-specific antibodies after western blotting. Ponceau S Red staining (P.R.) was used as a loading control. B, 2D-BN-PAGE of 1.6% digitonin-solubilized thylakoids isolated from wild-type L*er* and oe*CURT1A* plants grown under darkness, GL, and HL. Antibodies specific for CURT1A were used to detect CURT1A-containing protein complexes after separation in the second dimension by SDS-PAGE. The major protein complexes separated by BN-PAGE are numbered and represent PSII supercomplexes (1), PSI-LHCI-pLHCII (2), PSI-LHCI (3), Cyt b_6f dimer (4), and LHCII trimer (5). CURT1A signals corresponding to higher oligomeric complexes are highlighted by red rectangles. LMW, Low molecular weight.

conducted a tetrazolium staining assay to assess seed viability. The data obtained demonstrate a reduced viability of *curt1abcd* embryos compared with both wild-type and oe*CURT1A* lines (Fig. 4C).

Lack of CURT1 Affects Photosynthesis and Thylakoid Plasticity under Natural Environmental Conditions

To elucidate potential causes for the significant decrease in *curt1abcd* plant fitness under natural growth conditions, the physiological status of wild-type, *curt1abcd*, and oe*CURT1A* plants was assessed by PAM fluorometry, transmission electron microscopy (TEM) analysis, and studies of thylakoid protein composition. Differences observed in photosynthetic parameters for oe*CURT1A* and *curt1abcd* compared with the wild type were similar to those seen under controlled light conditions (Fig. 1A). While *curt1abcd* plants displayed significant decreases in F_v/F_m, Φ_{II}, and NPQ and an increase in 1-qL to levels comparable to those normally seen under light intensities intermediate between GL and HL, oe*CURT1A* plants showed wild-type-like values (Fig. 5A), suggesting that an excess of CURT1A does not preclude effective regulation of photosynthesis.

As previous studies suggest that the accumulation of photosynthetic proteins can vary significantly between plants grown under NC and CC (Mishra et al., 2012), the relative amounts of CURT1 proteins were determined (Fig. 5B). Under natural light conditions, an ~2-fold up-regulation of CURT1A (relative to controlled GL conditions) was observed in the wild type, while in oe*CURT1A*, an ~4-fold accumulation was noted (Fig. 5B). CURT1C was up-regulated ~2-fold in both the wild type and oe*CURT1A*, in comparison with the wild type, grown under controlled GL conditions. Surprisingly, when plants were grown under natural environmental conditions, CURT1B amounts increased almost 4-fold in both the wild type and oe*CURT1A*. However, no differential expression in CURT1B or CURT1C was detected between the wild type and oe*CURT1A* under natural environmental conditions.

TEM analyses of chloroplast cross sections showed differences in grana stack properties, with plants grown under NC showing a significantly reduced height (2- to 5-fold) compared with images taken under CC, while grana diameters changed only marginally between CC and NC within the respective genotypes (Fig. 5C; Supplemental Table S1). As a decrease in grana diameter is assumed to be functionally relevant under HL conditions (Herbstová et al., 2012), this lack of

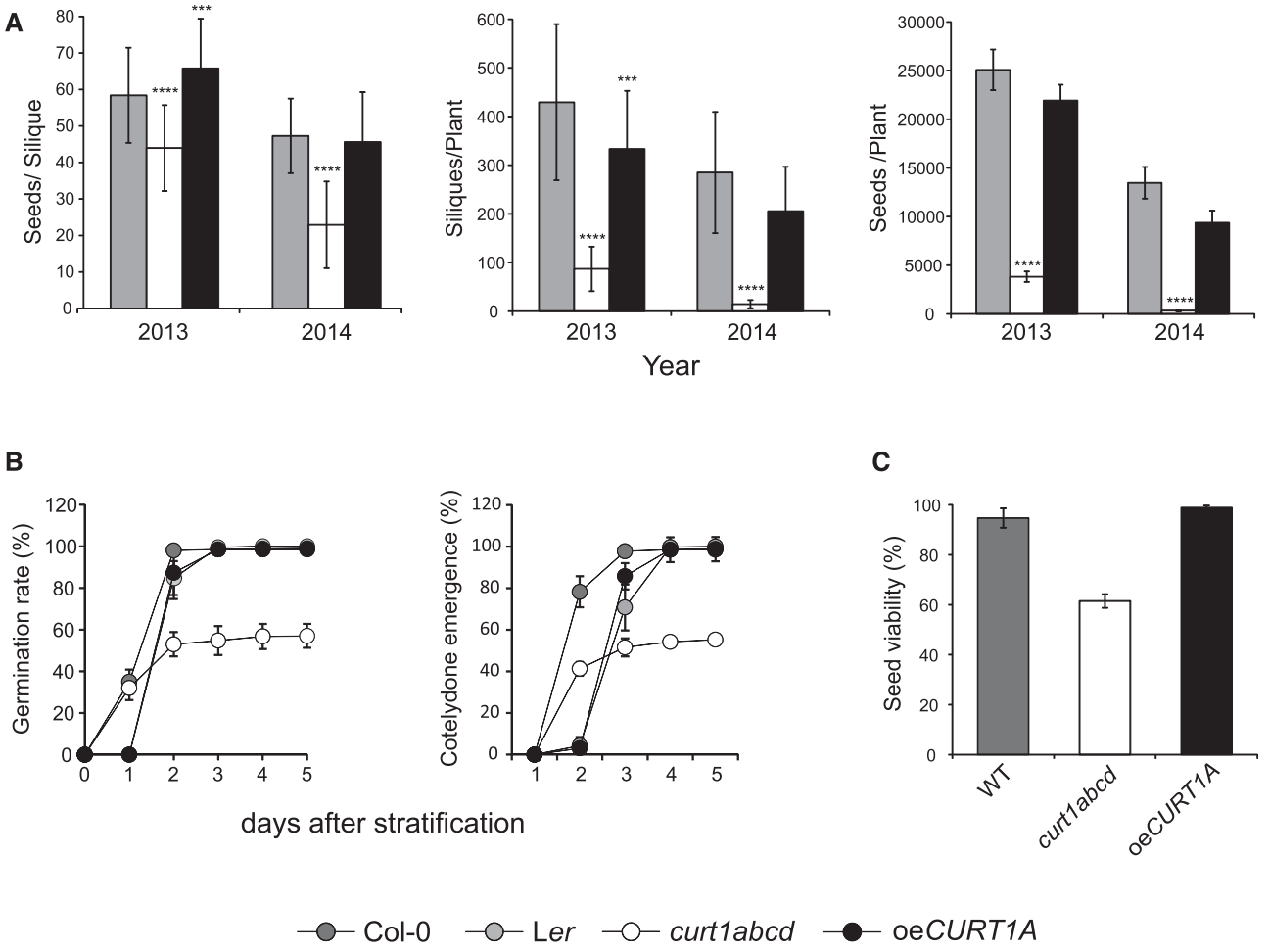

Figure 4. Lack of CURT1 reduces overall plant fitness and seed quality. A, Fitness of Arabidopsis wild-type, *curt1abcd*, and oe*CURT1A* plants as indicated by seed filling of siliques, silique formation, and overall seed production in two consecutive years of field trials (2013 and 2014). Left, Number of seeds per silique. Middle, Number of siliques per plant. Right, Total number of seeds, calculated from the number of siliques per plant and seeds per silique. Data are means ± SE; $n \geq 32$. B, Germination rates (left) and cotyledon emergence rates (right) of Arabidopsis seeds derived from wild-type (Col-0 and L*er*), *curt1abcd*, and oe*CURT1A* plants cultivated jointly to ensure equal developmental conditions for the seeds (50 seeds per experiment; $n = 6$). C, Seed viability test was performed from the same batch of seeds as described in B using the tetrazolium assay (100 seeds each experiment, $n = 3$). WT, Wild type. A two-sample Student's *t* test analysis ($P = 0.05$) was performed to determine the level of statistical significance; *P* values are represented by star code (***$P = 0.0001$–0.001 and ****$P < 0.0001$).

adjustment in *curt1abcd* might represent a major factor in impairing its fitness.

Finally, the composition of the major photosynthetic complexes within the thylakoid membrane was analyzed by BN-PAGE and 2D-BN-PAGE (Supplemental Fig. S3). Under NC, the patterns of assembled photosynthetic complexes in the wild type, *curt1abcd*, and oe*CURT1A* were comparable to those observed for the wild type under CC (Supplemental Fig. S3, A–D). Here, only the PSI-LHCI band appeared to be weaker in both oe*CURT1A* and *curt1abcd* compared with the wild type (Supplemental Fig. S3A). Regarding CURT1 complex assembly, the samples of oe*CURT1A* taken under NC showed significant amounts of HMW CURT1 complexes in comparison with the respective wild-type samples (Supplemental Fig. S3B). This suggests that moderate rather than HL intensities prevailed at the time of sampling, which is compatible with the corresponding photosynthetic parameters and TEM images (Figs. 1A and 5, A and C).

DISCUSSION

CURT1-Dependent Thylakoid Membrane Plasticity Is Critical for Efficient Photosynthetic Performance and Plant Fitness under Adverse and Variable Growth Conditions

The strong conservation of the characteristic ultrastructure of thylakoids, with its domains of appressed and nonappressed membranes (grana and stroma

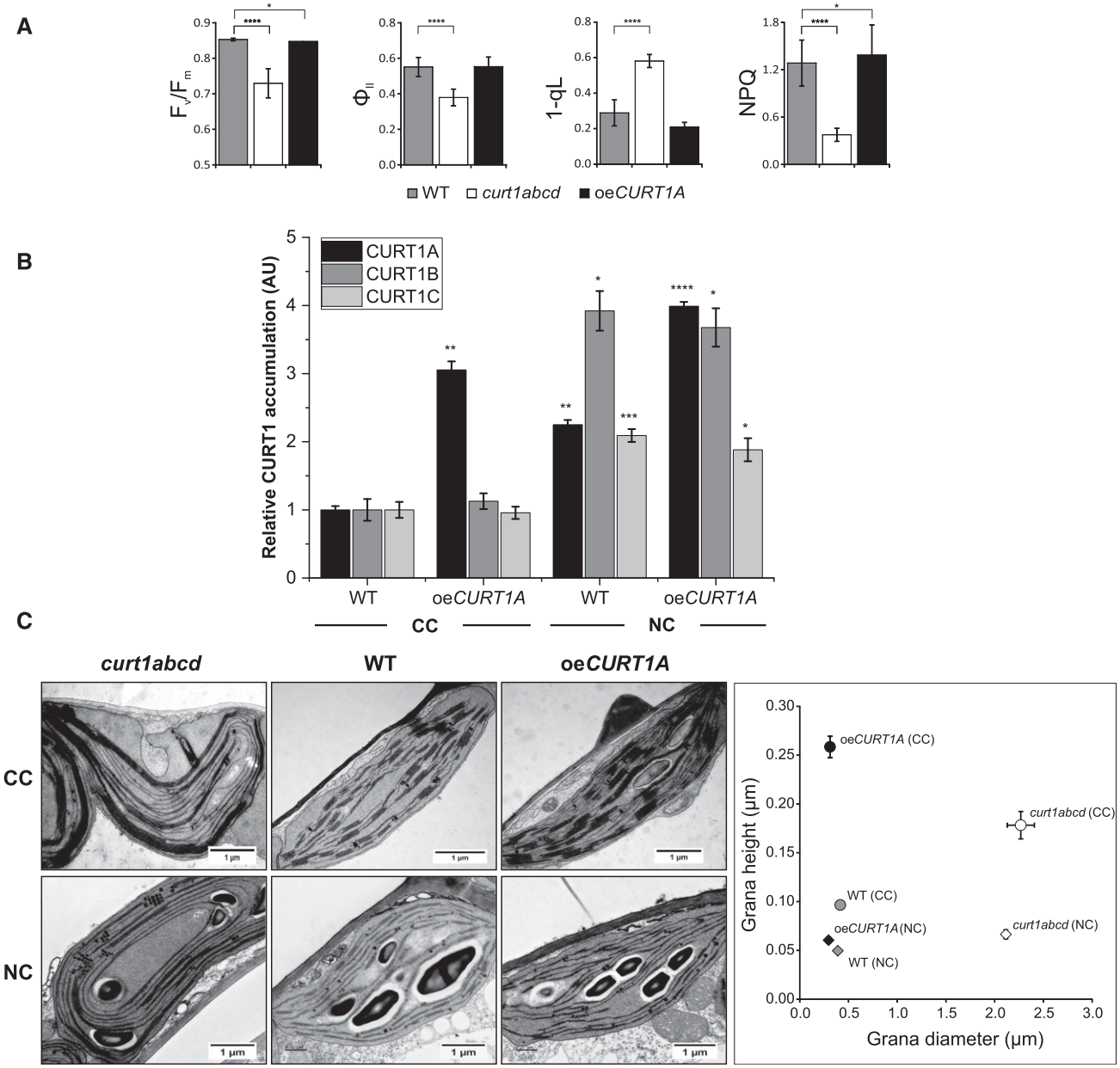

Figure 5. CURT1 influences photosynthesis and thylakoid plasticity under natural environmental conditions. A, The photosynthetic parameters F_v/F_m, Φ_{II}, NPQ, and 1-qL were determined for Arabidopsis wild-type (WT), *curt1abcd*, and oe*CURT1A* lines after growth under NC ($n = 7$). B, Bar diagram showing the relative levels of CURT1 proteins in thylakoid membrane preparations derived from Arabidopsis wild-type and oe*CURT1A* plants grown under NC and CC. Relative quantitation is based on immunoblots using antibodies specific for CURT1A, CURT1B, and CURT1C. For A and B, bars represent average values ± SE ($n \geq 5$). A two-sample Student's *t* test analysis ($P = 0.05$) was performed to determine the level of statistical significance; *P* values are represented by star code (*$P = 0.01$–0.05; **$P = 0.001$–0.01; ***$P = 0.0001$–0.001; and ****$P < 0.0001$). AU, Arbitrary units. C, Comparison of TE micrographs of chloroplast from Arabidopsis grown under NC and CC. Representative TEM images show chloroplasts from Arabidopsis (NC) wild-type, *curt1abcd*, and oe*CURT1A* lines taken at the same growth stage as the measurements shown in A. The scatterplot at right shows the diameter (*x* axis) and height (*y* axis) of grana stacks in Arabidopsis wild-type, *curt1abcd*, and oe*CURT1A* plants grown either under NC or CC light conditions. Average values ± SE are presented ($n \geq 30$). *P* values indicating the statistical significance of the differences in grana stacking between the genotypes are provided in Supplemental Table S2.

lamellae), among higher plants raises the question of its functional implications, especially with respect to photosynthetic processes (Anderson and Andersson, 1988; Allen and Forsberg, 2001; Mullineaux, 2005). Even though various mutant lines have been described that show an altered thylakoid architecture (Dörmann et al., 1995; Meurer et al., 1998; Gao et al., 2006; Kwon and Cho, 2008; Cui et al., 2011), these are usually

accompanied by severe defects in development and their photosynthetic apparatus, making them unsuitable for studying the specific impact of structural alterations of the thylakoid membrane on photosynthesis. Previously, the CURT1 protein family was identified, and both a dearth and a surfeit of these proteins (in *curt1abcd* and oe*CURT1A* mutant lines, respectively) were shown to perturb thylakoid ultrastructure specifically, essentially without affecting the thylakoid lipid-protein composition (Armbruster et al., 2013).

We report here an extensive study of the effects of various controlled lighting regimes and natural, fluctuating growth conditions on photosynthetic properties, plant growth, and fitness using mutants that lack (*curt1abcd*) or overproduce (oe*CURT1A*) CURT1 proteins involved in thylakoid membrane bending. Under essentially all growth conditions tested, oe*CURT1A* and *curt1abcd* plants showed reduced growth compared with the wild type, which was especially pronounced under adverse light conditions like short-day, LL, HL, and fluctuating light conditions (Supplemental Fig. S1). Under challenging and fluctuating environments (e.g. HL and field conditions), only the photosynthetic efficiency of *curt1abcd* plants was affected significantly (Figs. 1 and 5A). These observations can be explained by the apparent inability of *curt1abcd* plants to adjust the diameter of their grana stacks to wild-type-like dimensions under variable light conditions (Fig. 5C), a property reported previously to be important for the efficient operation of regulatory processes, such as state transitions (Kyle et al., 1984; Chuartzman et al., 2008) and PSII repair (D1 turnover; Fristedt et al., 2009; Herbstová et al., 2012). Photosynthetic regulatory mechanisms like state transitions and D1 turnover rely heavily on optimized protein diffusion processes to efficiently redistribute protein complexes like LHCII and PSII assembly states between grana core and stroma lamellae (Goral et al., 2010; Johnson et al., 2011; Herbstová et al., 2012; Kirchhoff, 2014a, 2014b; Yamamoto, 2016). In the case of the *curt1abcd* mutant, the increase in grana diameter also increases the diffusion distances of these proteins and ultimately impairs the actual processes, such as incomplete state 1-state 2 shift of antennae proteins during state transitions (Fig. 1B) or retarded D1 degradation under HL exposure (Fig. 1D; Supplemental Fig. S2). In the case of oe*CURT1A*, grana diameter-determined diffusion distances do not limit the regulatory processes as such, indicated by an even faster D1 degradation in lincomycin-treated oe*CURT1A* leaves (Figs. 1D and 6; Supplemental Fig. S2). This leads us to the assumption that the observed perturbations in the PSII repair cycle of oe*CURT1A* are of a different nature from thylakoid hyperbending, potentially imposing restrictions on the reassembly of functional PSII and its migration back into the grana core.

In summary, we speculate that a lack of thylakoid plasticity and the ability to adjust diffusion distances between stacked and unstacked membrane regions, as in the case of *curt1abcd*, becomes critical under variable and adverse light conditions that require a tight orchestration of electron and protein transport processes across the thylakoid membrane to maintain a high photosynthetic capacity (Fig. 6). Upon GL or HL exposition, we assume that CURT1 complexes disassemble, thereby enhancing thylakoid plasticity and decreasing grana diameter (Figs. 3B and 5C). Consequently, this facilitates PSII disassembly and D1 degradation as well as the movement of LHCII from PSII to PSI (state transitions; Fig. 6).

A general reduction in photosynthetic efficiency under variable NC further explains the severe reduction in plant fitness seen in the case of *curt1abcd* and reflected in the actual production of seeds under NC (Fig. 4A).

One can only speculate why oe*CURT1A* plants show a reduction in plant growth even though normal photosynthesis activity is maintained (Fig. 1C). The fact that oe*CURT1A* seeds tend to germinate with a certain delay (Fig. 4B) might account to some extent for this, and the effect was partially alleviated when RGRs were considered (Table I). Besides potential positional effects, the fact that oe*CURT1A* was generated in the Arabidopsis L*er* ecotype might have further resulted in an underestimation of the actual leaf size, due to a slightly inward-curled leaf shape seen in this accession. Also, pleiotropic effects not related to photosynthesis could account for the observed reduction in plant growth of oe*CURT1A*, as CURT1A overaccumulates systemically due to the 35S promoter. Further studies will be needed to address this issue in the future.

CURT1-Dependent Thylakoid Plasticity Is Regulated by Changes in the Oligomeric States Rather Than Protein Amount

Prior to this study, the molecular relationship between the increase in membrane bending and the increased protein amount of CURT1 in oe*CURT1A* was elusive. Similar to *curt1abcd*, oe*CURT1A* plants showed no significant alteration in the composition of their thylakoid pigment-protein complexes compared with the wild type, irrespective of the growth conditions (Fig. 2A; Supplemental Fig. S3). Interestingly, even though a mutual dependency in accumulation was demonstrated for CURT1 proteins when single or multiple CURT1 proteins were knocked out (Armbruster et al., 2013), overexpression of CURT1A in the presence of the other CURT1 proteins (oe*CURT1A*) led to a slight decrease in the expression of CURT1B and CURT1C, rather than to compensatory up-regulation to maintain a particular stoichiometry of complex subunits, at least when grown under GL (Figs. 2B and 3A). This suggests that CURT1A alone is sufficient for the increase in thylakoid membrane curvature in oe*CURT1A* cultivated under GL, which supports the notion that CURT1A possesses an intrinsic membrane-bending capacity, as shown previously in in vitro proteoliposome assays (Armbruster et al., 2013). Ectopic expression of CURT1A in planta in a CURT1-depleted

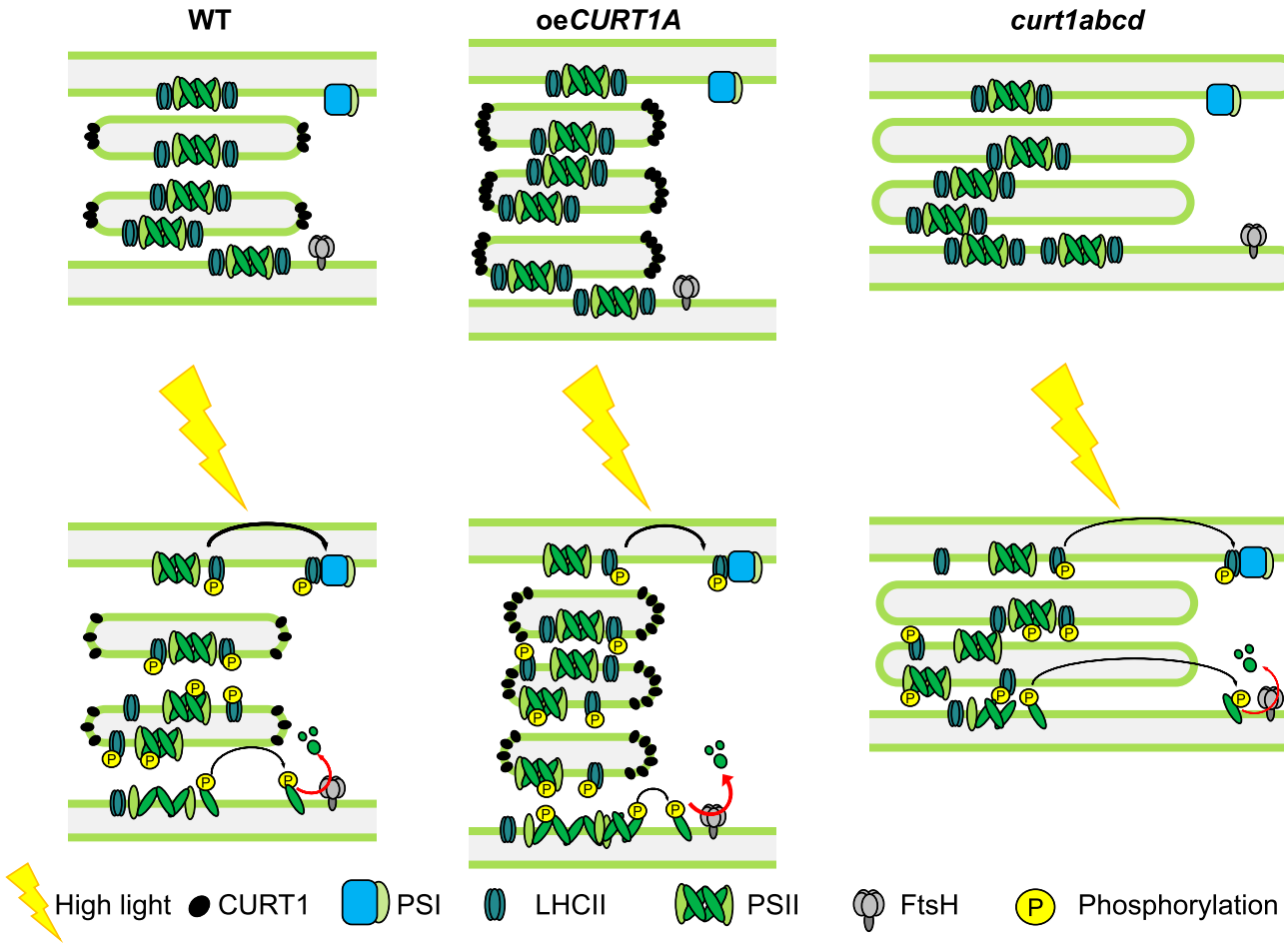

Figure 6. Proposed operation of CURT1 activity and consequences of its absence or overexpression. In the dark, a larger fraction of CURT1 complexes is present in high oligomeric states. Upon growth or HL exposition, CURT1 complexes disassemble and enhance grana plasticity as well as decrease grana diameter, promoting PSII disassembly, D1 degradation, and the movement of LHCII from PSII to PSI (state transitions). In *curt1abcd* plants, a lack of CURT1 proteins negatively affects thylakoid plasticity, thereby delaying the movement of LHCII antenna from PSII to PSI (transition from state 1 to state 2) and hampering D1 degradation. In contrast, overexpression of CURT1A leads to a reduced grana diameter and, thus, allows for a faster movement of D1 from grana to stroma lamellae and enhanced D1 degradation. However, this as such does not improve PSII repair. It is tempting to speculate that CURT1A-induced membrane hyperbending causes steric restrictions within the thylakoid membrane and affects the reassembly of PSII and its migration back into the grana core. Red arrows indicate D1 degradation, and black arrows indicate either PSII or LHCII migration. WT, Wild type.

mutant background also was able to partially restore thylakoid membrane bending and grana formation (Fig. 2C).

To better understand the discrepancy between the two types of structural thylakoid alteration in *curt1abcd* and oe*CURT1A* with respect to photosynthesis and plant fitness, CURT1 complex formation was monitored in wild-type and oe*CURT1A* plants under different short-term light exposures. In general, oe*CURT1A* plants showed a larger proportion of HMW CURT1 complexes compared with the wild type, whereas HMW CURT1 complexes were gradually destabilized with increasing light intensities, leading to a shift to lower-order CURT1 oligomers in both the wild type and oe*CURT1A* (Fig. 3B). Interestingly, CURT1 protein amounts were not affected by the short-term light conditions (Fig. 3A), which suggests a light intensity-dependent regulation of CURT1 complex formation, most likely at the posttranslational level. This could explain the fact that oe*CURT1A* plants retain the ability to actively regulate photosynthetic processes by altering thylakoid plasticity, which *curt1abcd* plants have lost (Fig. 6). Considering that CURT1 proteins can be reversibly phosphorylated (Armbruster et al., 2013) and that certain chloroplast protein kinases like STN8 are activated under increasing light intensities (Vainonen et al., 2005; Wunder et al., 2013), it is tempting to speculate that CURT1 complex stability is regulated via posttranslational modifications such as reversible protein phosphorylation.

CONCLUSION

Under natural or adverse growth conditions, depletion of CURT1 with concomitant impairment of the ability to adjust grana diameter has negative effects on both photosynthetic efficiency and regulatory photosynthetic mechanisms and, consequently, on plant growth and seed development. We suggest that intrinsic membrane-bending capacity resides within CURT1A, which is sufficient to restore thylakoid membrane curvature in planta. Therefore, thylakoid membrane plasticity mediated by CURT1 is critical for plant fitness and plays an important role in fine-tuning photosynthesis under challenging growth conditions. To gain a more comprehensive understanding of the molecular mechanism behind CURT1-mediated thylakoid membrane plasticity, future studies need to elucidate (1) the structure-function relation of potential CURT1 domains and (2) the role of reversible phosphorylation of CURT1 proteins, especially during acclimation to fluctuating environmental conditions.

MATERIALS AND METHODS

Plant Materials

In this study, the Arabidopsis (*Arabidopsis thaliana*) ecotypes L*er* and Col-0 were used as the wild-type control. The oe*CURT1A*, *curt1abc*, and *curt1abcd* lines have been described previously (Armbruster et al., 2013). To generate 35S:CURT1A *curt1abc* plants, the mature *CURT1A* sequence was amplified from Arabidopsis cDNA, using primers that included *attB* flanking sites (5′-GGGGACAAGTTTGTACAAAAAAGCAGGCTTCACCATGGCGATATCAGTAGCA-3′ and 5′-GGGGACCACTTTGTACAAGAAAGCTGGGTGCTATTCGCTTCCTGCGAT-3′) for direct cloning of the PCR fragment into the Gateway entry vector pDONR201 and subsequently into the destination vector pB7YWG2.0. Here, the *CURT1A* stop codon was retained to prevent the translation of an eYFP tag (Karimi et al., 2005; https://gateway.psb.ugent.be/). Arabidopsis (*curt1abc*) plants were transformed with the resulting construct using the floral dipping method as described previously (Clough and Bent, 1998).

Cultivation Conditions and Growth Measurement

Plants were grown in climate chambers under different light intensities and daylengths. Plants grown under long-day (16 h of light/8 h of dark), intermediate-day (12 h of light/12 h of dark), and short-day (8 h of light/16 h of dark) conditions were exposed to GL (120 μmol photons m^{-2} s^{-1}) during the light period. HL (900 μmol photons m^{-2} s^{-1}, 12 h of light/12 h of dark) conditions were realized using a special Hg lamp (Osram Powerstar HQIBT-D/400W). To compare the growth rates of wild-type plants with those of the different mutants under various light conditions, images of plants were taken once per week starting 2 weeks after planting. ImageJ software was used to calculate leaf areas (Abràmoff et al., 2004).

Growth Conditions during Fluctuating Light Measurements

Plants were grown on a 12-h/12-h light/dark photoperiod under either 75 μmol photons m^{-2} s^{-1} (control light) or 25 μmol photons m^{-2} s^{-1} (LL) from fluorescent tubes. Fluctuating light conditions were generated by superimposing 20-s flashes of 1,000 μmol photons m^{-2} s^{-1} white LED light on control light every 5 min during the relevant light period. Growth measurements were started when the total projected leaf area of plants was about 5 cm^2 ($n > 13$, each genotype). Counting from the day of seed sowing, *curt1abcd* plants reached this stage 1 week after the wild type (Col-0). The leaf area data were fitted to an exponential growth curve to calculate RGR (% d^{-1}).

PAM Measurements

The PAM 101/103 system was used to determine F_v/F_m, Φ_{II}, NPQ, and 1-qL as described before (Varotto et al., 2000). Five to seven plants were dark adapted for 15 min, and detached leaves were exposed subsequently to actinic light (37, 129, or 1,031 μmol photons m^{-2} s^{-1}) for 10 min to determine the photosynthetic parameters $F_v/F_m = (F_m - F_0)/F_m$, $\Phi_{II} = (F_m - F_s)/F_m'$, NPQ = $(F_m - F_m')/F_m'$, and 1-qL = $1 - (F_0'/F_s)(F_m' - F_s)/(F_m' - F_0')$ (Kramer et al., 2004).

Quenching of chlorophyll fluorescence due to qT was measured as reported earlier (Pribil et al., 2010). In brief, dark-adapted leaves were illuminated for 15 min with red light (35 μmol photons m^{-2} s^{-1}) to determine the maximum fluorescence in state 2 (F_m2). Then, state 1 was induced by exposure to far-red light (level 20 in the Dual-PAM setting) for 15 min, and F_m1 was recorded. qT was calculated according to the following equation: $qT = (F_m1 - F_m2)/F_m2$.

77K Measurements

Leaves of 4-week-old Arabidopsis wild-type (Col-0) and mutant (oe*CURT1A* and *curt1abcd*) plants were incubated under far-red light, promoting state 1, for 2 h followed by incubation under LL (80 μmol photons m^{-2} s^{-1}), promoting state 2, for 1 h. For each genotype and biological replicate, two mature rosette leaves were frozen after 2 h of far-red light as well as 30 and 60 min of LL treatment and stored at −80°C. The leaf samples were crushed and homogenized in the buffer (20 mM HEPES, pH 7.9, 300 mM sorbitol, 2.5 mM EDTA, 10 mM NH_4HCO_3, 2 mM sodium ascorbate, and 0.1% [w/v] BSA). The homogenate corresponds to 5 μg mL^{-1} chlorophyll and was used to measure the 77K fluorescence emission spectrum between 670 and 770 nm using an excitation wavelength of 435 nm. The emission spectra were recorded at 1 nm s^{-1}, keeping the bandwidth of 5 nm for both excitation and emission and normalized at 693 nm to compare the fluorescence emission peak deriving from PSI. All spectra represent averages of three biological replicates with five individual readings per replicate.

Photoinhibition (D1 Turnover) Assay

To assess D1 turnover rates in L*er*, *curt1abcd*, and oe*CURT1A* plants, F_v/F_m was measured after a short exposure to HL. Preceding treatments with lincomycin and water were performed as described previously (Fristedt et al., 2009) with minor modifications. More specifically, detached leaves with petioles were submersed in water or 1 mM lincomycin solution and incubated in the dark at 4°C for 16 h followed by a 3-h exposure to HL. Saturating light pulses (5,000 μmol photons m^{-2} s^{-1}) were applied in 0.5- or 1-h intervals to determine F_v/F_m after 15 min of dark adaptation.

Thylakoid Isolation, SDS-PAGE, and Western-Blot Analyses

Leaves from 4-week-old plants were harvested, and thylakoid membranes were prepared as described (Bassi et al., 1985). Thylakoid amounts were normalized on the basis of chlorophyll concentration (Porra, 2002). Thylakoid samples equivalent to 4 to 5 μg of chlorophyll were solubilized in SDS loading buffer and separated by SDS-PAGE (15% [w/v] acrylamide) as described (Schagger and von Jagow, 1987).

Proteins were transferred onto a PVDF membrane, and western blotting was performed according to the manufacturer's instructions (Millipore). If not stated otherwise, primary antibodies (e.g. against D1 and CURT1 proteins) were obtained from Agrisera. Protein amounts were quantified by the software Image Lab (Bio-Rad) by analyzing the intensities of protein signals.

2D-BN-PAGE

All experimental steps were carried out at 4°C, according to the procedure described previously (Armbruster et al., 2013). For native PAGE analysis, thylakoid samples equivalent to 100 μg of chlorophyll were solubilized in buffer (750 mM 6-aminocaproic acid, 5 mM EDTA, and 50 mM NaCl) containing 1.6% (w/v) digitonin for 1 h on a rotary wheel. After centrifugation at 16,000*g* for 1 h, solubilized pigment-protein complexes were fractionated by nondenaturing BN-PAGE as described previously (Schagger and von Jagow, 1991). SDS-PAGE in the second dimension was performed as before (Armbruster et al., 2010).

TEM Analysis

Explants of leaves from Arabidopsis were collected for TEM analysis. Sample preparation was performed as described previously (Armbruster et al., 2013). All steps were performed at 25°C. Briefly, leaves were cut into small squares (around 1 × 1 mm) and immediately fixed with 2.5% glutaraldehyde in 0.1 M sodium cacodylate buffer (pH 7) for 2 h. After two washes with cacodylate buffer, the leaves were postfixed with 1% osmium tetroxide for 2 h. The leaves were then washed with MilliQ water, dehydrated in acetone, and embedded in Spurr's low-viscosity resin. Ultrathin sections (60 nm) were prepared using a diamond knife and mounted on pioloform-coated copper grids. The sections were postfixed with uranyl acetate and lead citrate. Electron micrographs of NC samples were taken using a JEM 1230 (JEOL). Electron microscopy of the remaining samples was performed as described previously (Armbruster et al., 2013).

Seed Germination, Cotyledon Emergence, and Seed Viability Assays

Arabidopsis seeds were surface sterilized with 2% (v/v) bleach and washed four times with sterile water. Seeds of Col-0, L*er*, *curt1abcd*, and oe*CURT1A* were sown on 0.5× MS-Phytagel (Sigma-Aldrich) containing 1% (w/v) Suc and stratified for 2 d in the dark at 4°C. The seeds were exposed to 100 μmol photons m^{-2} s^{-1} for 5 d under long-day (16 h of light/8 h of dark) conditions at 21°C. Seed germination was defined as rupturing of the seed coat (testa) by the root, while cotyledon emergence was defined as the emergence of the cotyledons from the seed. Seed viability was determined using the tetrazolium method as described previously (Verma and Majee, 2013).

Field Trial Conditions

Field experiments were performed over two consecutive years (2013 and 2014) in the designated area outside of Umeå University in northern Sweden as described previously (Külheim et al., 2002; Frenkel et al., 2008). Seeds of wild-type, *curt1abcd*, and oe*CURT1A* plants were sown indoors on May 31 in 2013 and 2014 and grown for 3 weeks under controlled climate-chamber conditions. Afterward, plants were transferred to pots and initially placed outdoors in a shaded area for acclimation. After 3 to 4 d, the plants were exposed to direct sunlight and grown to maturity in the field in a randomized arrangement. To quantify plant fitness, five unopened siliques were collected from each plant to determine the average number of seeds per silique. All remaining siliques were counted, and fitness was assessed by multiplying the average number of seeds in each silique by the average number of siliques per plant. A second batch of plants was grown from mid-August to mid-September 2014 for PAM fluorometry, TEM analysis, and biochemical studies. Samples from the second batch were taken on September 22 at an ambient temperature of around 9°C and a maximum solar radiation of approximately 400 W m^{-2}.

Accession Numbers

The sequence data from this article can be found in The Arabidopsis Information Resource or GenBank/EMBL database under the following accession numbers: *CURT1A* (At4g01150), *CURT1B* (At2g46820), *CURT1C* (At1g52220), *CURT1D* (At4g38100), *LHCB1* (At1g29930), *PSAA* (AtCg00350), *PSAB* (AtCg00340), *ATPB* (AtCg00480), *PSBA/D1* (AtCg00020), and *PETB/Cytb*$_6$ (AtCg00720).

Supplemental Data

The following supplemental materials are available.

Supplemental Figure S1. Effects of a lack and a surfeit of CURT1 on photosynthesis and plant growth in plants cultivated under GL and on different photoperiods.

Supplemental Figure S2. D1 degradation kinetics in detached leaves of wild-type, *curt1abcd*, and oe*CURT1A* lines during HL exposure.

Supplemental Figure S3. Photosynthetic protein composition and distribution under CC and NC in the wild type, *curt1abcd*, and *oeCURT1A*.

Supplemental Table S1. Statistical (Student's *t* test) analyses of grana stack dimensions.

ACKNOWLEDGMENTS

We thank James Behrendorff and Paul Hardy for critical reading of the article. Silvia Dobler is thanked for excellent technical support with TEM sample preparation. We thank the Center of Advanced Bioimaging, University of Copenhagen, for proving TEM facilities.

Received July 6, 2017; accepted January 12, 2018; published January 26, 2018.

LITERATURE CITED

Abràmoff MD, Magalhães PJ, Ram SJ (2004) Image processing with ImageJ. Biophoton Int **11:** 36–42

Albertsson P (2001) A quantitative model of the domain structure of the photosynthetic membrane. Trends Plant Sci **6:** 349–358

Allen JF, Forsberg J (2001) Molecular recognition in thylakoid structure and function. Trends Plant Sci **6:** 317–326

Allorent G, Osorio S, Vu JL, Falconet D, Jouhet J, Kuntz M, Fernie AR, Lerbs-Mache S, Macherel D, Courtois F, et al (2015) Adjustments of embryonic photosynthetic activity modulate seed fitness in Arabidopsis thaliana. New Phytol **205:** 707–719

Anderson JM (1986) Photoregulation of the composition, function, and structure of thylakoid membranes. Annu Rev Plant Physiol Plant Mol Biol **37:** 93–136

Anderson JM, Andersson B (1988) The dynamic photosynthetic membrane and regulation of solar energy conversion. Trends Biochem Sci **13:** 351–355

Anderson JM, Chow WS, De Las Rivas J (2008) Dynamic flexibility in the structure and function of photosystem II in higher plant thylakoid membranes: the grana enigma. Photosynth Res **98:** 575–587

Andersson B, Anderson JM (1980) Lateral heterogeneity in the distribution of chlorophyll-protein complexes of the thylakoid membranes of spinach chloroplasts. Biochim Biophys Acta **593:** 427–440

Armbruster U, Labs M, Pribil M, Viola S, Xu W, Scharfenberg M, Hertle AP, Rojahn U, Jensen PE, Rappaport F, et al (2013) *Arabidopsis* CURVATURE THYLAKOID1 proteins modify thylakoid architecture by inducing membrane curvature. Plant Cell **25:** 2661–2678

Armbruster U, Zühlke J, Rengstl B, Kreller R, Makarenko E, Rühle T, Schünemann D, Jahns P, Weisshaar B, Nickelsen J, et al (2010) The *Arabidopsis* thylakoid protein PAM68 is required for efficient D1 biogenesis and photosystem II assembly. Plant Cell **22:** 3439–3460

Bassi R, dal Belin Peruffo A, Barbato R, Ghisi R (1985) Differences in chlorophyll-protein complexes and composition of polypeptides between thylakoids from bundle sheaths and mesophyll cells in maize. Eur J Biochem **146:** 589–595

Chuartzman SG, Nevo R, Shimoni E, Charuvi D, Kiss V, Ohad I, Brumfeld V, Reich Z (2008) Thylakoid membrane remodeling during state transitions in *Arabidopsis*. Plant Cell **20:** 1029–1039

Clough SJ, Bent AF (1998) Floral dip: a simplified method for Agrobacterium-mediated transformation of Arabidopsis thaliana. Plant J **16:** 735–743

Cui YL, Jia QS, Yin QQ, Lin GN, Kong MM, Yang ZN (2011) The GDC1 gene encodes a novel ankyrin domain-containing protein that is essential for grana formation in Arabidopsis. Plant Physiol **155:** 130–141

Dekker JP, Boekema EJ (2005) Supramolecular organization of thylakoid membrane proteins in green plants. Biochim Biophys Acta **1706:** 12–39

Dörmann P, Hoffmann-Benning S, Balbo I, Benning C (1995) Isolation and characterization of an *Arabidopsis* mutant deficient in the thylakoid lipid digalactosyl diacylglycerol. Plant Cell **7:** 1801–1810

Frenkel M, Jänkänpää HJ, Moen J, Jansson S (2008) An illustrated gardener's guide to transgenic Arabidopsis field experiments. New Phytol **180:** 545–555

Fristedt R, Willig A, Granath P, Crèvecoeur M, Rochaix JD, Vener AV (2009) Phosphorylation of photosystem II controls functional macroscopic folding of photosynthetic membranes in *Arabidopsis*. Plant Cell **21:** 3950–3964

Gao H, Sage TL, Osteryoung KW (2006) FZL, an FZO-like protein in plants, is a determinant of thylakoid and chloroplast morphology. Proc Natl Acad Sci USA **103:** 6759–6764

Goral TK, Johnson MP, Brain AP, Kirchhoff H, Ruban AV, Mullineaux CW (2010) Visualizing the mobility and distribution of chlorophyll proteins in higher plant thylakoid membranes: effects of photoinhibition and protein phosphorylation. Plant J **62:** 948–959

Herbstová M, Tietz S, Kinzel C, Turkina MV, Kirchhoff H (2012) Architectural switch in plant photosynthetic membranes induced by light stress. Proc Natl Acad Sci USA **109:** 20130–20135

Johnson MP, Goral TK, Duffy CD, Brain AP, Mullineaux CW, Ruban AV (2011) Photoprotective energy dissipation involves the reorganization of photosystem II light-harvesting complexes in the grana membranes of spinach chloroplasts. Plant Cell **23:** 1468–1479

Karimi M, De Meyer B, Hilson P (2005) Modular cloning in plant cells. Trends Plant Sci **10:** 103–105

Khatoon M, Inagawa K, Pospísil P, Yamashita A, Yoshioka M, Lundin B, Horie J, Morita N, Jajoo A, Yamamoto Y, et al (2009) Quality control of photosystem II: thylakoid unstacking is necessary to avoid further damage to the D1 protein and to facilitate D1 degradation under light stress in spinach thylakoids. J Biol Chem **284:** 25343–25352

Kirchhoff H (2008) Molecular crowding and order in photosynthetic membranes. Trends Plant Sci **13:** 201–207

Kirchhoff H (2013a) Architectural switches in plant thylakoid membranes. Photosynth Res **116:** 481–487

Kirchhoff H (2013b) Structural constraints for protein repair in plant photosynthetic membranes. Plant Signal Behav **8:** e23634

Kirchhoff H (2014a) Diffusion of molecules and macromolecules in thylakoid membranes. Biochim Biophys Acta **1837:** 495–502

Kirchhoff H (2014b) Structural changes of the thylakoid membrane network induced by high light stress in plant chloroplasts. Philos Trans R Soc Lond B Biol Sci **369:** 20130225

Kramer DM, Johnson G, Kiirats O, Edwards GE (2004) New fluorescence parameters for the determination of QA redox state and excitation energy fluxes. Photosynth Res **79:** 209–218

Külheim C, Agren J, Jansson S (2002) Rapid regulation of light harvesting and plant fitness in the field. Science **297:** 91–93

Kwon KC, Cho MH (2008) Deletion of the chloroplast-localized AtTerC gene product in Arabidopsis thaliana leads to loss of the thylakoid membrane and to seedling lethality. Plant J **55:** 428–442

Kyle DJ, Ohad I, Arntzen CJ (1984) Membrane protein damage and repair: selective loss of a quinone-protein function in chloroplast membranes. Proc Natl Acad Sci USA **81:** 4070–4074

Meurer J, Plücken H, Kowallik KV, Westhoff P (1998) A nuclear-encoded protein of prokaryotic origin is essential for the stability of photosystem II in *Arabidopsis thaliana*. EMBO J **17:** 5286–5297

Mishra Y, Jänkänpää HJ, Kiss AZ, Funk C, Schröder WP, Jansson S (2012) Arabidopsis plants grown in the field and climate chambers significantly differ in leaf morphology and photosystem components. BMC Plant Biol **12:** 6

Mullineaux CW (2005) Function and evolution of grana. Trends Plant Sci **10:** 521–525

Mustárdy L, Garab G (2003) Granum revisited. A three-dimensional model: where things fall into place. Trends Plant Sci **8:** 117–122

Nevo R, Charuvi D, Tsabari O, Reich Z (2012) Composition, architecture and dynamics of the photosynthetic apparatus in higher plants. Plant J **70:** 157–176

Porra RJ (2002) The chequered history of the development and use of simultaneous equations for the accurate determination of chlorophylls a and b. Photosynth Res **73:** 149–156

Pribil M, Labs M, Leister D (2014) Structure and dynamics of thylakoids in land plants. J Exp Bot **65:** 1955–1972

Pribil M, Pesaresi P, Hertle A, Barbato R, Leister D (2010) Role of plastid protein phosphatase TAP38 in LHCII dephosphorylation and thylakoid electron flow. PLoS Biol **8:** e1000288

Schägger H, von Jagow G (1987) Tricine-sodium dodecyl sulfate-polyacrylamide gel electrophoresis for the separation of proteins in the range from 1 to 100 kDa. Anal Biochem **166:** 368–379

Schägger H, von Jagow G (1991) Blue native electrophoresis for isolation of membrane protein complexes in enzymatically active form. Anal Biochem **199:** 223–231

Shimoni E, Rav-Hon O, Ohad I, Brumfeld V, Reich Z (2005) Three-dimensional organization of higher-plant chloroplast thylakoid membranes revealed by electron tomography. Plant Cell **17:** 2580–2586

Vainonen JP, Hansson M, Vener AV (2005) STN8 protein kinase in *Arabidopsis thaliana* is specific in phosphorylation of photosystem II core proteins. J Biol Chem **280:** 33679–33686

Varotto C, Pesaresi P, Meurer J, Oelmüller R, Steiner-Lange S, Salamini F, Leister D (2000) Disruption of the Arabidopsis photosystem I gene psaE1 affects photosynthesis and impairs growth. Plant J **22:** 115–124

Verma P, Majee M (2013) Seed germination and viability test in tetrazolium (TZ) assay. Bio Protoc **3:** e884

Wunder T, Xu W, Liu Q, Wanner G, Leister D, Pribil M (2013) The major thylakoid protein kinases STN7 and STN8 revisited: effects of altered STN8 levels and regulatory specificities of the STN kinases. Front Plant Sci **4:** 417

Yamamoto Y (2016) Quality control of photosystem II: the mechanisms for avoidance and tolerance of light and heat stresses are closely linked to membrane fluidity of the thylakoids. Front Plant Sci **7:** 1136

Yoshioka-Nishimura M, Nanba D, Takaki T, Ohba C, Tsumura N, Morita N, Sakamoto H, Murata K, Yamamoto Y (2014) Quality control of photosystem II: direct imaging of the changes in the thylakoid structure and distribution of FtsH proteases in spinach chloroplasts under light stress. Plant Cell Physiol **55:** 1255–1265